

Numerical Simulation of Supersonic Compression Corners and Hypersonic Inlet Flows Using the RPLUS2D Code

Kamlesh Kapoor, Bernhard H. Anderson, and Robert J. Shaw
Lewis Research Center
Cleveland, Ohio

November 1994



National Aeronautics and
Space Administration

(NASA-TM-106580) NUMERICAL
SIMULATION OF SUPERSONIC
COMPRESSION CORNERS AND HYPERSONIC
INLET FLOWS USING THE RPLUS2D CODE
(NASA. Lewis Research Center) 14 p

N95-16038

Unclass

G3/02 0031422

NUMERICAL SIMULATION OF SUPERSONIC COMPRESSION CORNERS AND HYPERSONIC INLET FLOWS USING THE RPLUS2D CODE

Kamlesh Kapoor,* Bernhard H. Anderson, and Robert J. Shaw
National Aeronautics and Space Administration
Lewis Research Center
Cleveland, Ohio 44135

SUMMARY

A two-dimensional computational code, RPLUS2D, which was developed for the reactive propulsive flows of ramjets and scramjets, was validated for two-dimensional shock-wave/turbulent-boundary-layer interactions. The problem of compression corners at supersonic speeds was solved using the RPLUS2D code. To validate the RPLUS2D code for hypersonic speeds, it was applied to a realistic hypersonic inlet geometry. Both the Baldwin-Lomax and the Chien two-equation turbulence models were used. Computational results showed that the RPLUS2D code compared very well with experimentally obtained data for supersonic compression corner flows, except in the case of large separated flows resulting from the interactions between the shock wave and turbulent boundary layer. The computational results compared well with the experiment results in a hypersonic NASA P8 inlet case, with the Chien two-equation turbulence model performing better than the Baldwin-Lomax model.

INTRODUCTION

The performance of high-speed inlets is often significantly affected by the interaction between the shock wave and turbulent boundary layer. Shock-wave/boundary-layer interaction is one of the most difficult problems to solve numerically. The purpose of the present investigation is to test the capability of the RPLUS2D code to predict supersonic compression corners, and then to apply the code to a realistic high-speed inlet geometry.

The problem of supersonic compression corners was studied experimentally by Settles et al. (refs. 1 and 2), who obtained experiment data for two-dimensional compression corners of 8° , 16° , 20° , and 24° . The incoming boundary layer had an edge Mach number of 2.85 and a Reynolds number (Re_δ) of $1.7 \times 10^6/m$ based on boundary layer thickness.

The numerical simulation of supersonic compression corners has been carried out by many researchers (refs. 3 to 7), but success was limited to attached flow and with small separated flows. The accurate prediction of large, shock-induced separated flows is still a challenge. Although turbulence modeling in shock-wave/boundary-layer interaction has been the subject of many investigations (refs. 6 and 7) during the past few years, there is still considerable doubt as to the general validity of any particular turbulence model. Keeping this in mind, the RPLUS2D code was applied in various situations that ranged from a nonseparated (i.e., attached) flow situation (8° ramp) to a large, shock-induced separated flow (24° ramp).

The RPLUS2D code solves the full two-dimensional, Reynolds-averaged, Navier-Stokes equations. The Baldwin-Lomax (ref. 8) and Chien two-equation (ref. 9) turbulence models were used in this study. This report compares the computations performed for $M_0 = 2.85$, where $\alpha = 8^\circ$, 16° , 20° , and 24° , and where $Re_0 = 7.3 \times 10^7/m$ with the experiment data of Settles et al. (ref. 1).

*National Research Council—NASA Research Associate at NASA Lewis Research Center.

Cruise conditions of the NASA P8 inlet (ref. 10) are typical of a hypersonic air-breathing vehicle and so it was selected as a test case of hypersonic inlet flows for this study. The free-stream Mach number was 7.4, the free-stream unit Reynolds number (Re_o) was $8.86 \times 10^6/m$, and the free-stream total temperature (Tt_o) was 811 K. Wedge and cowl surfaces were cooled to provide a uniform surface temperature of $0.375 Tt_o$. The NASA P8 inlet has been studied numerically by many investigators (refs. 11 to 13). Recently, Kapoor et al. (ref. 14) compared the abilities of various turbulence models to predict hypersonic inlet flows when applied to the NASA P8 inlet. The geometry of the inlet model tested is shown in figure 1. The inlet model was a Mach 7.4, rectangular, mixed-compression design with exiting supersonic flow and had an internal compression ratio of 8; it is referred to as the P8 inlet. The purpose of the present investigation was to test the capability of the RPLUS2D code to predict hypersonic inlet flows.

SYMBOLS

M	Mach number
p	static pressure
P_p	Pitot pressure
Pt	total pressure
Re	Reynolds number
Tt	total temperature
u_τ	friction velocity, $\sqrt{\tau_w / \rho_w}$
X	axial distance from the leading edge of the centerbody
XREF	inlet cowl height
y^+	law-of-the-wall coordinate, $u_\tau Y / \nu_w$
Y	vertical distance from the centerbody
α	ramp angle
δ	boundary layer thickness
ν	kinematic viscosity
ρ	density
τ	shear stress

Subscripts:

- ϕ tunnel free-stream condition
- τ shear stress
- ω evaluated at wall

RPLUS2D CODE

The RPLUS2D code was developed to study mixing and chemical reaction in the flowfield of ramjets and scramjets (refs. 15 and 16). It employs both an implicit finite volume and a lower, upper-symmetric, successive overrelaxation (LU-SSOR) scheme which solves the full two-dimensional, Reynolds-averaged, Navier-Stokes equations and the species transport equations in a fully coupled manner. Yoon and Jameson (refs. 17 and 18) initially developed the LU-SSOR scheme for nonreacting flows and used extensive testing to show that it was very robust and efficient for transonic and supersonic flows. We feel that the RPLUS2D code has the potential to provide a substantial speed advantage over the Navier-Stokes codes in current use.

A switching parameter in the RPLUS2D code allows it to be used for either a reacting or nonreacting flow. In this study, air was treated as a single species, nonreacting gas.

Supersonic Compression Corner Flows

Experimental background, the method used for computational solution, computational results, and a discussion of the results of this test of the RPLUS2D code capability to predict supersonic compression corners are included herein.

Experimental background.—Experiments were conducted in the Princeton University 20 by 20 cm-high Reynolds-number, supersonic wind tunnel. Compression corner models of 8°, 16°, 20°, and 24° were tested on the wall of the wind tunnel (ref. 1). The uniform free-stream conditions were: Mach number of 2.85, stagnation pressure of 6.8 atm, stagnation temperature of 268 K, and average free-stream unit Reynolds number of $7.3 \times 10^7/\text{m}$.

The incoming turbulent boundary layer for the four compression-corner experiments had an overall thickness (δ) of about 2.3 cm.

Method of solution.—The computational grid used in this study was 151 by 91. The grid was uniform in the X direction. To resolve the viscous layer, the grid lines were packed close to the ramp wall with hyperbolic tangent functions such that the first grid line was located at a y^+ of approximately 5.0 away from the wall.

The incoming boundary-layer profile was approximated by calculating the development of a turbulent boundary layer on a flat plate to the point where the boundary-layer thickness was equal to the experimental value.

The computations were performed on the CRAY-YMP supercomputer at NASA Lewis Research Center. The RPLUS2D code typically required a total of 10 min of CPU time to achieve global convergence for the Baldwin-Lomax model, which increased by approximately 20 percent when the Chien two-equation model was used.

Results and discussion.—Computational results are presented in the form of surface pressure distributions on the ramps. Skin friction calculations carried out previously by Lee (ref. 19) were shown to be consistent with the experiment data. Therefore, only ramp surface pressure distributions are presented in this report.

Figure 2(a) shows the surface pressure distribution for an 8° ramp for both the Baldwin-Lomax and the Chien two-equation turbulence models. As seen in the figure, the numerical results compare very well with the experiment data. Both turbulence models predict almost identical results.

Figure 2(b) presents the surface pressure distribution for a 16° ramp. The experimentally obtained results show a small region of separated flow just upstream of the corner. The computational results compare fairly well with the experiment data. Both turbulence models predicted nearly similar results.

Surface pressure distribution for a 20° ramp angle is illustrated in figure 2(c). The experimentally derived results show significant flow separation with the length of the separated region extended for about 65 percent of the incoming boundary layer thickness. The computational results compare fairly well with the experiment data. The Chien turbulence model performed better than the Baldwin-Lomax model.

Surface pressure distribution for a 24° ramp compression corner is outlined in figure 2(d). The results of the experiment show a massive flow separation with the extent of the separated region slightly more than twice the incoming boundary layer thickness. The computational results did not compare very well with the experiment data. Both the Baldwin-Lomax and Chien two-equation turbulence models failed to predict shock-induced, large separated flows.

It is evident from this study that the RPLUS2D code results compare reasonably well with the experiment data, except in the case of large separated flows resulting from the shock-wave/boundary-layer interaction. It is still a challenge to accurately predict such flows; more effort is required to develop better turbulence models suitable for this problem.

Hypersonic Inlet Flows

Included in this section of the paper are the experimental background, method used for computational solution, computational results, and a discussion of the results of the RPLUS2D code application to a realistic hypersonic inlet flow.

Experimental background.—An experimental investigation was conducted at the NASA Ames 3.5-ft Hypersonic Wind Tunnel to determine the internal flow characteristics of a typical inlet on a hypersonic air-breathing vehicle operating at cruise conditions. The P8 inlet cowl height (XREF) was 18.33 cm, forebody length was 81.28 cm, overall length was 136.2 cm, and width was 35.56 cm. A 6.5° forebody wedge was designed to produce an oblique shock wave that passed just outside the cowl lip and delivered flow at Mach 6.0 at the entrance of the inlet. The wedge was cooled to provide a uniform surface temperature of $0.357 T_{t_0}$, where the free-stream total temperature (T_{t_0}) was 811 K. The free-stream unit Reynolds number (Re_0) was $8.86 \times 10^6/m$. The experimentally determined laminar-turbulent transition point on the centerbody was approximately 40 percent of the distance between the wedge leading edge and the inlet entrance. The laminar-turbulent transition point in the cowl boundary layer was approximately halfway between the cowl leading edge and the throat station. Details of the experiments can be found in reference 10.

This realistic inlet geometry, with strong viscous-inviscid interactions and the availability of extensive experiment data, provided an excellent opportunity to verify the ability of the numerical algorithm and turbulence models to predict a hypersonic inlet flow field.

Method of solution.—The computational grid used in this study was 221 by 91 and nonuniform in the X direction. The grid was packed on both ends from the wedge leading edge to the cowl leading edge and was also geometrically stretched from the cowl leading edge to the outflow boundary. To resolve the viscous layer, the grid lines were packed close to the centerbody and cowl walls using hyperbolic tangent functions such that the first grid line was located at a y^+ of approximately 4.0 away from the walls.

The laminar-turbulent transition points on the ramp and cowl surfaces for the Baldwin-Lomax model were manually simulated from experiments by setting eddy viscosity equal to zero for laminar flows.

The computations were performed on the CRAY-YMP supercomputer at NASA Lewis Research Center. The RPLUS2D code typically required a total of 15 min of CPU time to achieve global convergence for the Baldwin-Lomax model, which increased by approximately 20 percent when the Chien two-equation model was used.

Results and discussion.—The performance of a hypersonic inlet is significantly affected by the interaction of the shock waves and turbulent boundary layers. The interaction between the inlet cowl-lip shock and centerbody turbulent-boundary-layer, in particular, requires careful analysis since the centerbody contours are often designed to cancel the cowl-lip shock. The internal contours of the P8 inlet model were designed to provide cancellation of the cowl shock at the centerbody and an isentropic compression to the throat. Nevertheless, a reflected shock was found experimentally, which further interacted with the cowl and centerbody boundary layers upstream of the throat. This significantly affected the flow structure at the inlet throat. The present computations were able to capture these flow characteristics.

The computed density, pressure, and Mach number contours for the Chien turbulence model are shown in figure 3. The contours obtained from the Baldwin-Lomax turbulence model were essentially similar. Figure 3 clearly illustrates that the cowl shock, after interacting with the centerbody turbulent-boundary-layer, was reflected downstream and interacted with the cowl turbulent-boundary-layer. The cowl shock was then reflected from the cowl and interacted again with the centerbody turbulent-boundary-layer before it left the inlet.

Further computed results are presented in the form of surface pressure distributions on the centerbody and cowl of the inlet model, and the Pitot pressure and total temperature distributions at many stations from the inlet entrance to the throat of the inlet. The results are compared with the corresponding experiment data from reference 10.

The surface pressure distributions on the centerbody are shown in figure 4. The axial distances are nondimensionalized with the inlet cowl height. The surface pressure distributions indicate that the computed results predict the location of the interaction of the cowl shock wave with the centerbody turbulent-boundary-layer slightly upstream as compared with the experiment.

The results obtained using the Baldwin-Lomax model show the existence of a separation bubble on the centerbody in the immediate region of cowl-lip-shock/centerbody-boundary-layer interaction. The existence of the separation bubble was confirmed by the presence of negative velocities in the separated region as shown in the insert of figure 4. No separation was reported in the experiment. Kapoor et al. (ref. 14) also reported the presence of a separation bubble when they used the Baldwin-Lomax model in the PARC2D code. On the other hand, the Chien model does not show the presence of a separation bubble and is able to successfully simulate the complex flow field resulting from the interaction between the cowl shock and the centerbody turbulent-boundary-layer.

The pressure distributions on the cowl surface are presented in figure 5. The computed results show the flow compression and impingement of the reflected shock wave on the cowl. The expansion ahead of the reflected shock impingement, which is a feature associated with the shock-wave/boundary-layer interaction on the centerbody, is also visible in the computed results. The Chien two-equation turbulence model performs better than the Baldwin-Lomax model in predicting cowl surface pressure distributions.

The computational and experimentally derived Pitot pressures where X/X_{REF} equals 5.67, a station upstream of the intersection of the cowl shock with the centerbody, are shown in figure 6. The agreement of the computed results with the experiment data is generally good. The steep rise in the Pitot pressure where Y/X_{REF} equals 0.15 is due to the presence of the cowl shock. The results from the design analysis in reference 10 and the boundary-layer thicknesses on the centerbody and cowl surfaces obtained from the experiments are also marked in figure 6. The Chien two-equation model compares fairly well with the experiment data.

All of the present computational results overpredicted the Pitot pressures in the central region of the inlet. A recent AGARD report (ref. 13) noted that no one has ever matched the experiment data using the tunnel conditions stated in reference 10. The various computational results tend to agree with one another, but do not match the experiment data. The AGARD report further suspected that the conditions stated in reference 10 were different in some way from the conditions that were actually present in the tunnel. It should be noted that because of the high sensitivity of hypersonic flows, even small variations in the upstream flow field would lead to larger variations downstream.

The total temperature profile where $X/XREF$ equals 5.67 is presented in figure 7. The experimentally obtained total temperature ratio is less than 1.0 because it was not corrected for the uncertainties in other measurements (ref. 10). The comparison of the computed results with experiment data is generally good. The Chien two-equation model compares well with the experiment data, particularly near the centerbody.

The pitot pressure and total temperature distributions where $X/XREF$ equals 6.09, the intersection point of cowl shock with centerbody, are presented in figures 8 and 9, respectively. The computational results compare qualitatively well with experiment data.

The pitot pressure and total temperature distributions where $X/XREF$ equals 6.37, a station just downstream of the reflection of the cowl shock from the centerbody, are presented in figures 10 and 11, respectively. Figure 10 illustrates that the centerbody boundary layer of the experiment has been compressed by the reflecting shock wave and is thinner than at the previous station. The reflected shock wave emerges from the boundary layer where $Y/XREF$ equals 0.025, as shown by the break in the curve. The computations are able to detect the emerging shock wave, but the magnitude and location of the emerging shock differs for both turbulence models. Design analysis from reference 10 is also presented. The comparison of total temperatures with experiment data is good, as shown in figure 11.

The pitot pressures and total temperatures where $X/XREF$ equals 6.65, a station upstream of the inlet throat, are shown in figures 12 and 13, respectively. The comparison of pitot pressures and total temperatures with the experimentally derived data is qualitatively good.

The inlet performance was obtained in terms of pitot pressure, total temperature, and Mach number distributions at the throat. Figure 14 depicts a large variation of the pitot pressure distribution across the throat height due to the presence of the reflected shock wave. Results of the design analysis from reference 10 are also shown in figure 14. The total temperature distribution at the throat is shown in figure 15 and the Mach number profile at the throat is presented in figure 16. The computed results are in fair agreement with the experimentally derived data.

CONCLUDING REMARKS

The RPLUS2D code was validated for two-dimensional shock wave and turbulent boundary layer interactions. Supersonic flow over compression corners and hypersonic flow in the NASA P8 inlet were numerically simulated. Both the Baldwin-Lomax and Chien two-equation turbulence models were investigated in this study.

The computational results show that the RPLUS2D code compares very well with experimentally derived data for supersonic compression corner flows for the nonseparated and small separated flows, but it fails in the case of large shock-induced separated flows.

The computational results from the RPLUS2D code compare reasonably well with experimentally derived results when applied to the hypersonic NASA P8 inlet. Our conclusion from this study is that the Chien two-equation turbulence model performs better than the Baldwin-Lomax model for hypersonic inlet flows.

ACKNOWLEDGMENTS

This research was conducted while the first author held a National Research Council Research Associateship at NASA Lewis Research Center. The authors are thankful to Dr. Jinho Lee of Sverdrup Technology, Inc., NASA Lewis Research Center Group, for providing the RPLUS2D code.

REFERENCES

1. Settles, G.S.; Fitzpatrick, T.J.; and Bogdonoff, S.M.: Detailed Study of Attached and Separated Compression Corner Flowfields in High Reynolds Number Supersonic Flow. *AIAA J.*, vol. 17, no. 6, 1979, pp. 579-585.
2. Settles, G.S.; Vas, I.E.; and Bogdonoff, S.M.: Details of a Shock-Separated Turbulent Boundary Layer at a Compression Corner. *AIAA J.*, vol. 14, no. 12, 1976, pp. 1709-1715.
3. Shang, J.S.; Hankey, W.L., Jr.: Numerical Solution for Supersonic Turbulent Flow over a Compression Ramp. *AIAA J.*, vol. 13, no. 10, 1975, pp. 1368-1374.
4. Shang, J.S.; Hankey, W.L., Jr.; and Law, C.H.: Numerical Simulation of Shock Wave-Turbulent Boundary Layer Interaction. *AIAA J.*, vol. 14, no. 10, 1976, pp. 1451-1457.
5. Hung, C.M.; and MacCormack, R.W.: Numerical Simulation of Supersonic and Hypersonic Turbulent Compression Corner Flows. *AIAA J.*, vol. 15, no. 3, 1977, pp. 410-416.
6. Visbal, M.; and Knight, D.D.: The Baldwin-Lomax Turbulence Model for Two-Dimensional Shock Wave/Boundary Layer Interactions. *AIAA J.*, vol. 22, no. 7, 1984, pp. 921-928.
7. Homes, S.C.; and Squire, L.C.: Numerical Studies of Supersonic Flow Over a Compression Corner. *Aeronautical J.*, March 1992, pp. 87-95.
8. Baldwin, B.; and Lomax, H.: Thin-Layer Approximation and Algebraic Model for Separated Turbulent Flows. *AIAA Paper*, Jan. 1978, pp. 78-257.
9. Chien, K.Y.: Predictions of Channel Flow and Boundary Layer Flow with Low Reynolds Number Turbulence Model. *AIAA J.*, vol. 20, no. 1, 1982, pp. 33-38.
10. Gnos, A.V.; Watson, E.C.; Seebaugh, W.R.; Sanator, R.J.; and DeCarlo, J.P.: Investigation of Flow Fields Within Large-Scale Hypersonic Inlet Models. *NASA TN-D-7150*, 1973.
11. Knight, D.D.: Numerical Simulation of Realistic High-Speed Inlet Using the Navier-Stokes Equations. *AIAA J.*, vol. 15, no. 11, 1977, pp. 1583-1589.
12. Ng, W.F.; Ajmani, K.; and Taylor, A.C., III: Turbulence Modeling in a Hypersonic Inlet. *AIAA J.*, vol. 27, no. 10, 1989, pp. 1354-1360.
13. Air Intakes for High Speed Vehicles. *AGARD AR-270*, Sept. 1991, pp. 183-201.
14. Kapoor, K.; Anderson, B.H.; and Shaw, R.J.: Comparative Study of Turbulence Models in Predicting Hypersonic Inlet Flows. *AIAA Paper 92-3098*, July 1992.
15. Shuen, J.S.; and Yoon, S.: Numerical Study of Chemically Reacting Flows Using a Lower-Upper Symmetric Successive Overrelaxation Scheme. *AIAA J.*, vol. 27, no. 12, 1989, pp. 1752-1760.
16. Yu, S.T.; Tsai, Y.-L. Peter; and Shuen, J.S.: Three-Dimensional Calculation of Supersonic Reacting Flows Using an LU Scheme. *AIAA Paper 89-0391*, Jan. 1989.
17. Yoon, S.; and Jameson, A.: An LU-SSOR Scheme for the Euler and Navier-Stokes Equations. *AIAA Paper 87-0600*, Jan. 1987.
18. Jameson, A.; and Yoon, S.: Lower-Upper Implicit Schemes with Multiple Grids for the Eulers Equations. *AIAA J.*, vol. 25, no. 7, 1987, pp. 929-935.
19. Lee, J.: An Analysis of Supersonic Flows with Low-Reynolds Number Compressible Two-Equation Turbulence Model Using Implicit Finite Volume Numerical Techniques Based on Lower-Upper Diagonal Decomposition. *AIAA Paper 94-0193*, Jan. 1994.

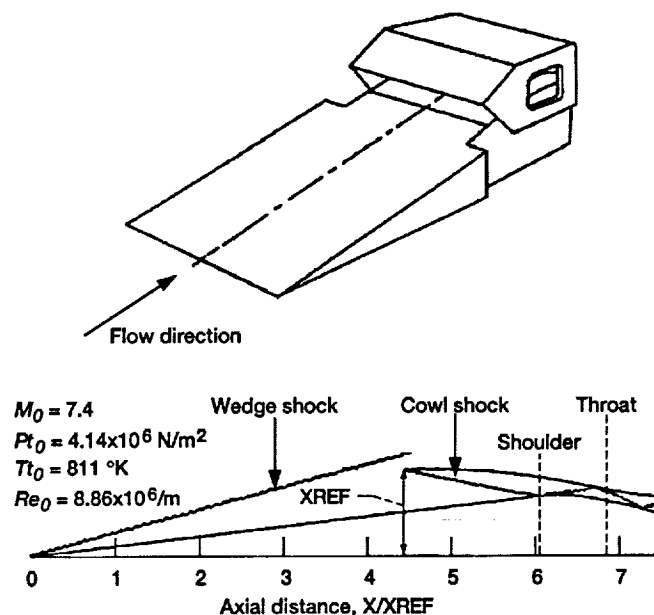


Figure 1.—Diagram of P8 inlet model.

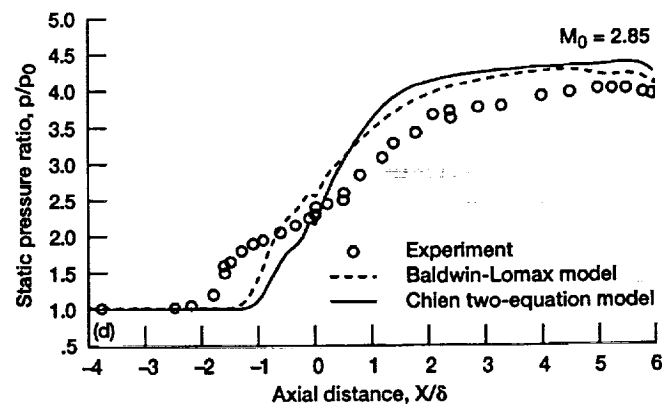
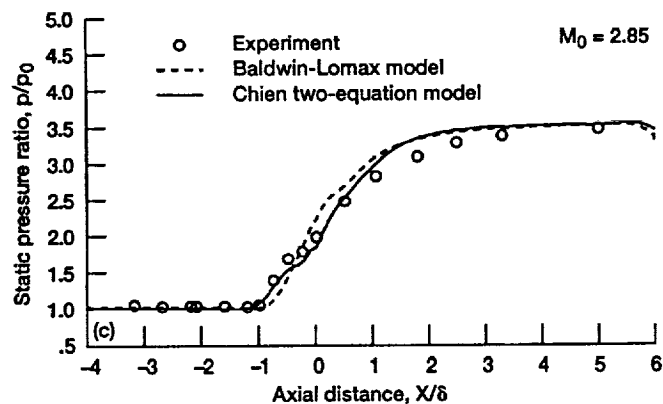
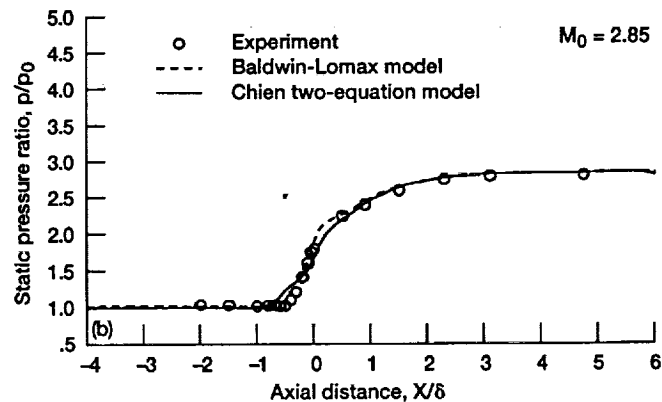
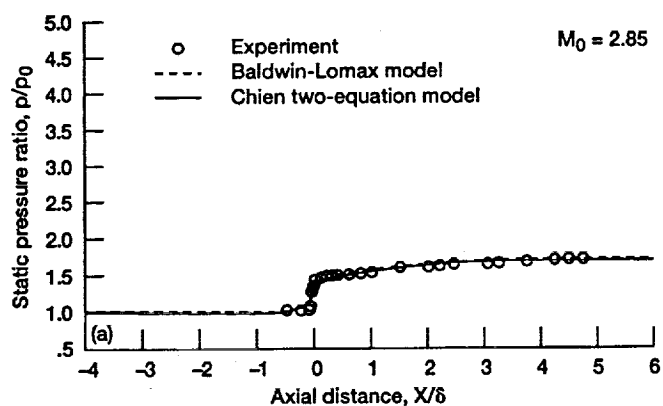
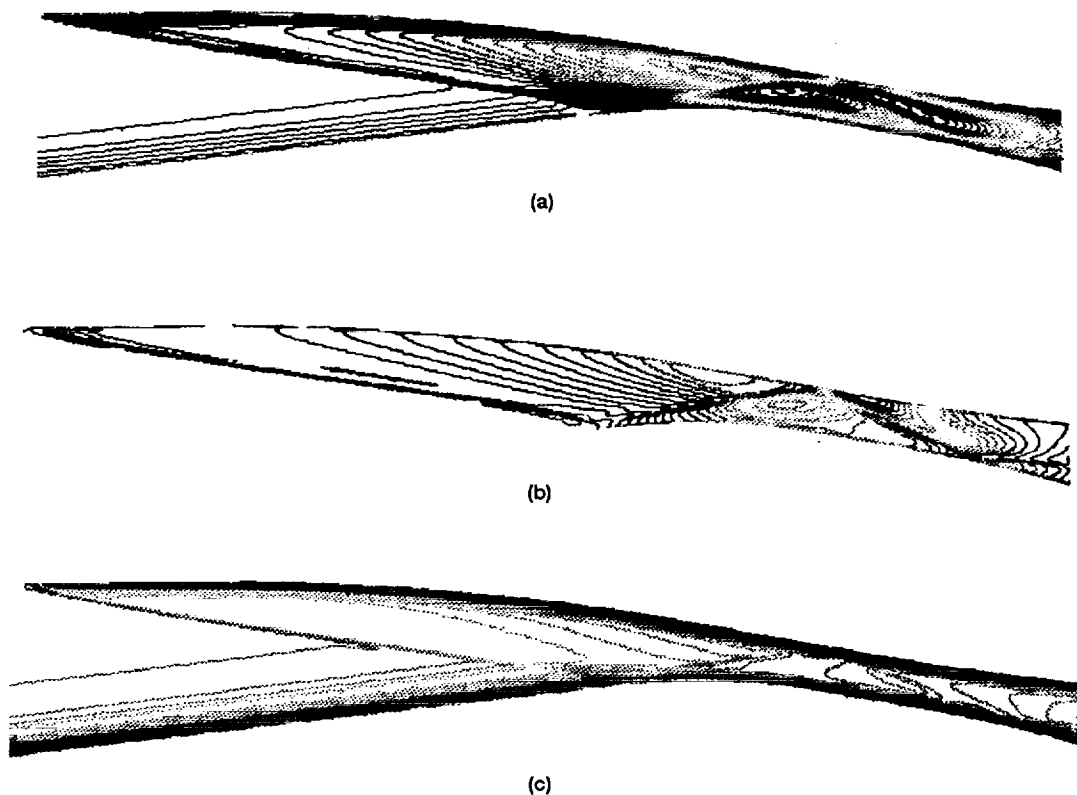


Figure 2.—Comparison of computed and experimentally determined pressure distribution for an inlet ramp in supersonic flow where (a) $\alpha = 8^\circ$, (b) $\alpha = 16^\circ$, (c) $\alpha = 20^\circ$, and (d) $\alpha = 24^\circ$.



(a) Density Contour Level	(b) Pressure Contour Level	(c) Mach number Contour Level
0.01000	0.00000	0.00000
0.02000	1000.000	0.20000
0.03000	2000.000	0.40000
0.04000	3000.000	0.60000
0.05000	4000.000	0.80000
0.06000	5000.000	1.00000
0.07000	6000.000	1.20000
0.08000	7000.000	1.40000
0.09000	8000.000	1.60000
0.10000	9000.000	1.80000
0.11000	10000.00	2.00000
0.12000	11000.00	2.20000
0.13000	12000.00	2.40000
0.14000	13000.00	2.60000
0.15000	14000.00	2.80000
0.16000	15000.00	3.00000
0.17000	16000.00	3.20000
0.18000	17000.00	3.40000
0.19000	18000.00	3.60000
0.20000	19000.00	3.80000
0.21000	20000.00	4.00000
0.22000	21000.00	4.20000
0.23000	22000.00	4.40000
0.24000	23000.00	4.60000
0.25000	24000.00	4.80000
0.26000	25000.00	5.00000
0.27000	26000.00	5.20000
0.28000	27000.00	5.40000
0.29000	28000.00	5.60000
0.30000	29000.00	5.80000
0.31000	30000.00	6.00000
0.32000	31000.00	6.20000
0.33000	32000.00	6.40000
0.34000		6.60000
0.35000		6.80000
0.36000		7.00000
0.37000		7.20000
0.38000		7.40000
0.39000		
0.40000		

Figure 3.—Typical (a) density, (b) pressure, and (c) Mach number contours for P8 inlet.

2024-01-01
2024-01-01

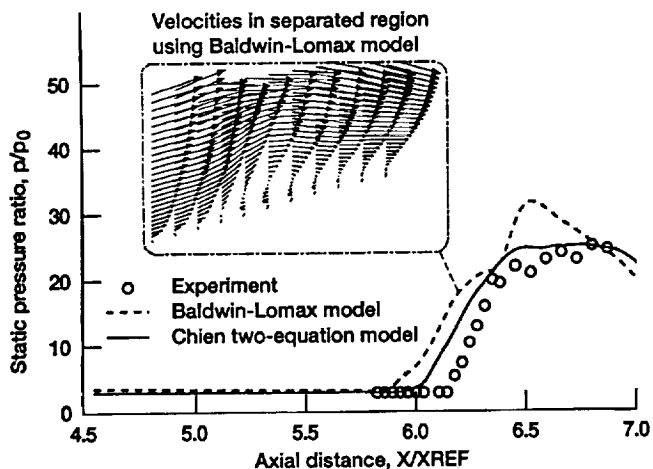


Figure 4.—Surface pressure distribution on the centerbody and velocity distribution in separated flow region.

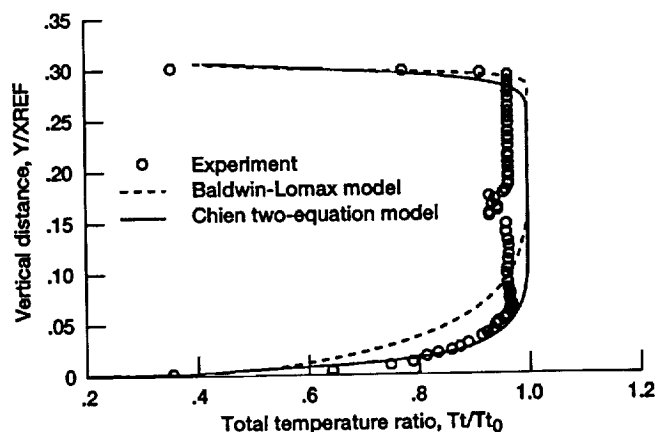


Figure 7.—Total temperature distribution where X/X_{REF} equals 5.67.

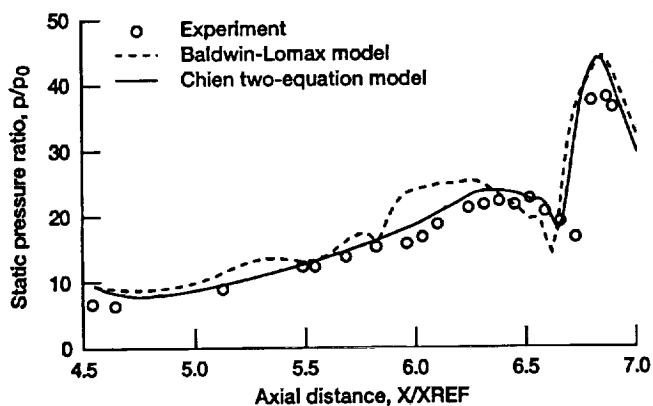


Figure 5.—Surface pressure distribution on the cowl.

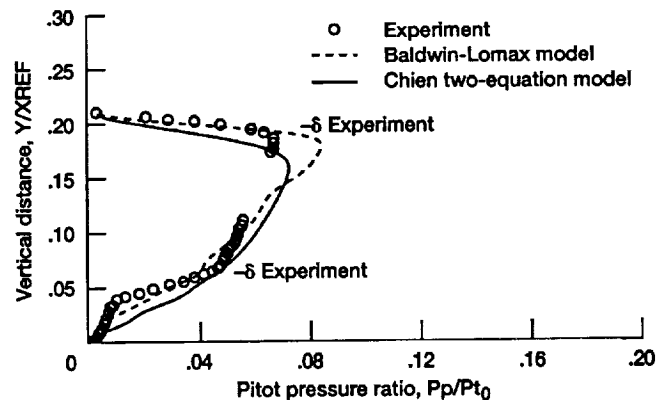


Figure 8.—Pitot pressure distribution where X/X_{REF} equals 6.09.

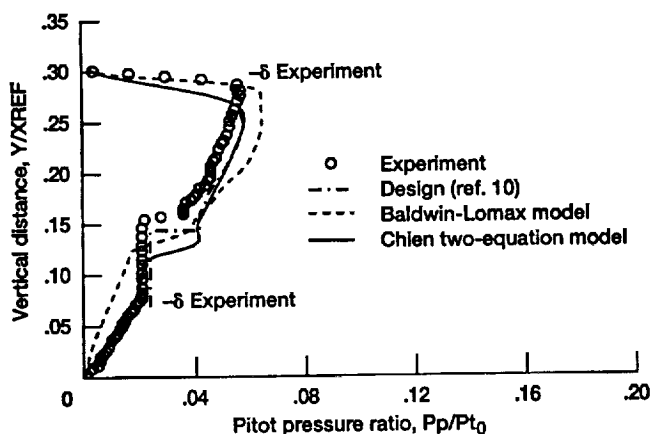


Figure 6.—Pitot pressure distribution where X/X_{REF} equals 5.67.

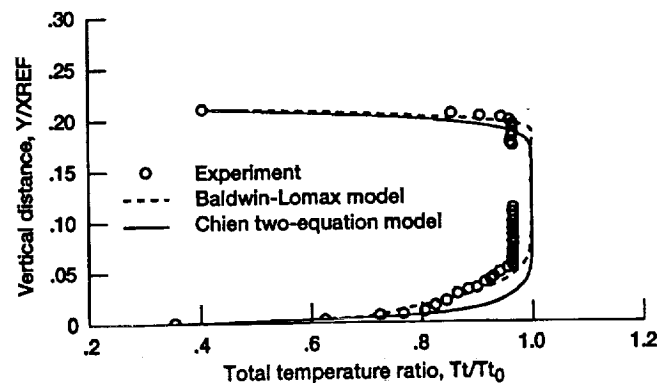


Figure 9.—Total temperature distribution where X/X_{REF} equals 6.09.

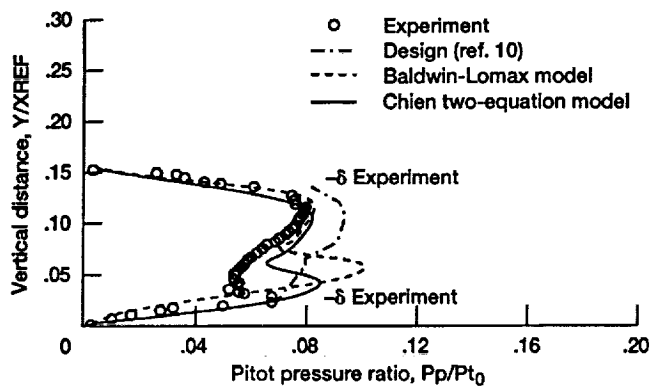


Figure 10.—Pitot pressure distribution where X/X_{REF} equals 6.37.

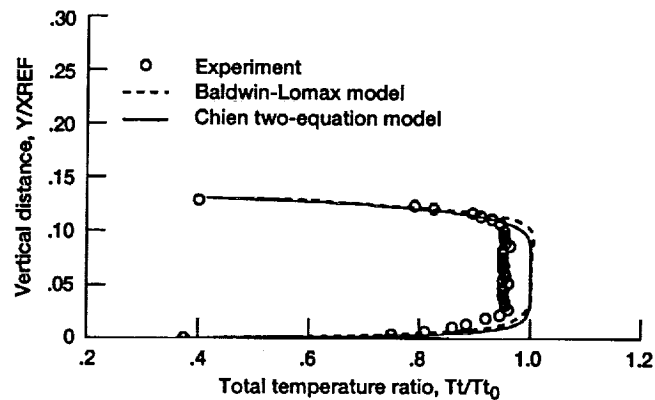


Figure 13.—Total temperature distribution where X/X_{REF} equals 6.65.

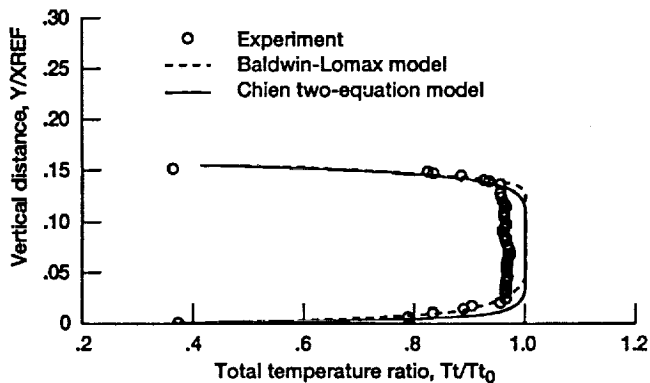


Figure 11.—Total temperature distribution where X/X_{REF} equals 6.37.

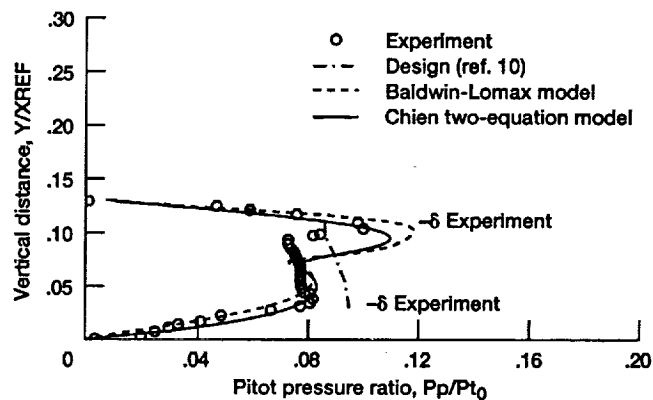


Figure 14.—Pitot pressure distribution at the throat.

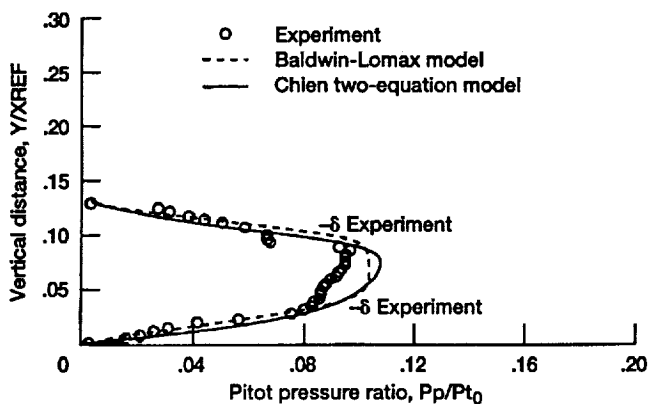


Figure 12.—Pitot pressure distribution where X/X_{REF} equals 6.65.

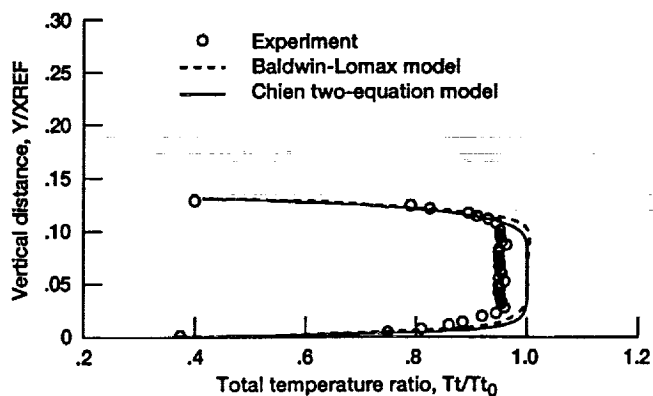


Figure 15.—Total temperature distribution at the throat.

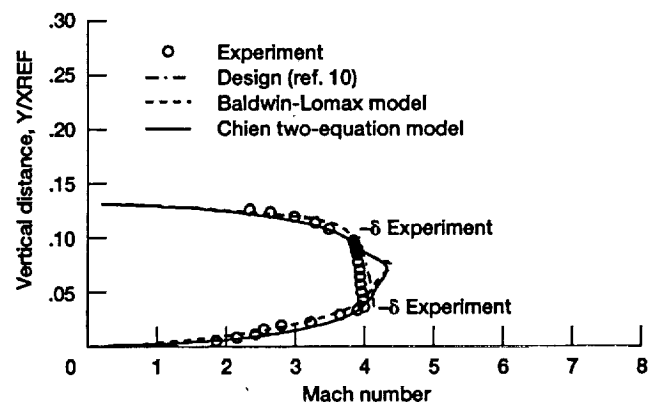


Figure 16.—Mach number distribution at the throat.

REPORT DOCUMENTATION PAGE			Form Approved OMB No. 0704-0188	
Public reporting burden for this collection of information is estimated to average 1 hour per response, including the time for reviewing instructions, searching existing data sources, gathering and maintaining the data needed, and completing and reviewing the collection of information. Send comments regarding this burden estimate or any other aspect of this collection of information, including suggestions for reducing this burden, to Washington Headquarters Services, Directorate for Information Operations and Reports, 1215 Jefferson Davis Highway, Suite 1204, Arlington, VA 22202-4302, and to the Office of Management and Budget, Paperwork Reduction Project (0704-0188), Washington, DC 20503.				
1. AGENCY USE ONLY (Leave blank)		2. REPORT DATE November 1994		3. REPORT TYPE AND DATES COVERED Technical Memorandum
4. TITLE AND SUBTITLE Numerical Simulation of Supersonic Compression Corners and Hypersonic Inlet Flows Using the RPLUS2D Code			5. FUNDING NUMBERS WU-537-02-23	
6. AUTHOR(S) Kamlesh Kapoor, Bernhard H. Anderson, and Robert J. Shaw				
7. PERFORMING ORGANIZATION NAME(S) AND ADDRESS(ES) National Aeronautics and Space Administration Lewis Research Center Cleveland, Ohio 44135-3191			8. PERFORMING ORGANIZATION REPORT NUMBER E-8840	
9. SPONSORING/MONITORING AGENCY NAME(S) AND ADDRESS(ES) National Aeronautics and Space Administration Washington, D.C. 20546-0001			10. SPONSORING/MONITORING AGENCY REPORT NUMBER NASA TM-106580	
11. SUPPLEMENTARY NOTES Kamlesh Kapoor, National Research Council—NASA Research Associate at Lewis Research Center; and Bernhard H. Anderson and Robert J. Shaw, NASA Lewis Research Center. Responsible person, Kamlesh Kapoor, organization code 2780, (216) 433-8295.				
12a. DISTRIBUTION/AVAILABILITY STATEMENT Unclassified - Unlimited Subject Category 02			12b. DISTRIBUTION CODE	
13. ABSTRACT (Maximum 200 words) A two-dimensional computational code, PRLUS2D, which was developed for the reactive propulsive flows of ramjets and scramjets, was validated for two-dimensional shock-wave/turbulent-boundary-layer interactions. The problem of compression corners at supersonic speeds was solved using the RPLUS2D code. To validate the RPLUS2D code for hypersonic speeds, it was applied to a realistic hypersonic inlet geometry. Both the Baldwin-Lomax and the Chien two-equation turbulence models were used. Computational results showed that the RPLUS2D code compared very well with experimentally obtained data for supersonic compression corner flows, except in the case of large separated flows resulting from the interactions between the shock wave and turbulent boundary layer. The computational results compared well with the experiment results in a hypersonic NASA P8 inlet case, with the Chien two-equation turbulence model performing better than the Baldwin-Lomax model.				
14. SUBJECT TERMS Shock wave; Turbulent boundary layer interactions			15. NUMBER OF PAGES 15	
			16. PRICE CODE A03	
17. SECURITY CLASSIFICATION OF REPORT Unclassified	18. SECURITY CLASSIFICATION OF THIS PAGE Unclassified	19. SECURITY CLASSIFICATION OF ABSTRACT Unclassified	20. LIMITATION OF ABSTRACT	

**National Aeronautics and
Space Administration
Lewis Research Center
21000 Brookpark Rd.
Cleveland, OH 44135-3191**

**Official Business
Penalty for Private Use \$300**

POSTMASTER: If Undeliverable — Do Not Return

